Analyzing the Evolutionary Characteristics of the Cluster of COVID-19 under Anti-contagion Policies

Pu Miao[1,2], Hu Tian[1,2], Xingwei Zhang[1,2], Saike He[1,2] , Xiaolong Zheng[1,2], Desheng Dash Wu[3,4] ,Daniel Zeng[1,2,3]
[1]The State Key Laboratory of Management and Control for Complex Systems, Institute of Automation, Chinese Academy of Sciences, Beijing 100190, China
[2]School of Artificial Intelligence, Chinese Academy of Sciences, Beijing 100190, China
[3]University of Chinese Academy of Sciences Beijing 100190, China
[4]Stockholm Business School, Stockholm University, SE-106 91 Stockholm, Sweden
{miaopu2018, tianhu2018,zhangxingwei2019,saike.he, xiaolong.zheng, dajun.zeng}@ia.ac.cn, dash@risklab.ca

***Abstract*—With the rampaging of Coronavirus disease 2019 (COVID-19) across the world, analyzing the dynamic characteristics and understanding the evolutionary patterns of clusters are becoming even more crucial for people and policymakers to make timely responses for avoiding injury caused by COVID-19. To solve the scarcity of the fine-grained spatio-temporal data, we construct a novel dataset about the spread of patients during the resurgent period of the COVID-19 epidemic at the Xinfadi Market in Beijing. Leveraging our self-build dataset, we analyze the evolutionary characteristics of the cluster of COVID-19 under anti-contagion policies and obtained some remarkable evolution patterns. These findings can provide significant insights for policymakers and researchers to understand the evolutionary characteristics regarding the cluster of COVID-19 and deploy effective anti-contagion policies.**

Keywords—complex network, epidemic, outbreak, COVID-19, epidemic spread network

I. INTRODUCTION

Governments around the world are responding to the coronavirus disease 2019 (COVID-19) pandemic, caused by severe acute respiratory syndrome coronavirus 2 (SARS-CoV-2) [1]. Due to the neglect of early intervention, the cluster of COVID-19 often causes a wide range of diffusion[2]. A convincing example is the different spread results between the Huanan seafood market in Wuhan and the Xinfadi market in Beijing. The former cluster of coronaviruses led to a pandemic in the Chinese mainland due to without early intervention, while the latter only spread in a small region. Because the modern world has never confronted this pathogen, nor deployed anti-contagion policies for the cluster of COVID-19 patients, it is crucial that study the dynamic characteristics and understand the evolutionary patterns of the cluster of COVID-19.

However, it is non-trivial to model the dynamic evolution of the cluster of COVID-19. Essentially, the evolution of the cluster of COVID-19 is a dynamic interaction process between people and locations. The difficulties are three-fold: (1) The fine-grained location data (e.g. street, community, and working place) is scarce. The geo-visualization project developed by the team of researchers of Johns Hopkins University can visualize the report cases on the level of countries, states, provinces, cities, or regions, but always based on a coarse-grained territorial logic. (2) The spread of COVID-19 involves the heterogeneous–homogeneous interaction between infected people and locations, which needs an appropriate modeling method. (3) The spread of COVID-19 contains a dynamic evolution process about the interaction between people and locations.

To analyze the evolutionary characteristics of the cluster of COVID-19, we construct a new dataset about the spread of patients during the resurgent period of the COVID-19 epidemic at the Xinfadi Market in Beijing. Since a cluster of COVID-19 has broken out in Beijing on June 11 and presented a certain trend of spread. The National Health Commission and Beijing Health Commission took some decisive anti-contagion policies such as closing restaurants or restricting travel, thereby slowing the spread of COVID-19 to a manageable rate. Based on the patient epidemiological investigation data published by the Beijing Health Commission, in this article, we extracted the confirmed COVID-19 patients and their historical location data.

To model the dynamic interaction of the confirmed COVID-19 patients and locations, we directly use the historical trajectories of confirmed COVID-19 patients to construct dynamic interaction networks. The dynamic interaction networks allow us to study the spread of COVID-19 and analyze its evolution patterns from both macro and micro perspectives. Complex network analysis [3], a powerful tool to model network data, plays an important role in many real-world applications and has shown promising results in various domains, including social network analysis [4, 5], security informatics[6], sociology [7, 8]. In public health, the complex network can also model the transmission of epidemics such the Dengue Fever [9, 10], influenza[11], SARS [12, 13].

Overall, the contributions of this paper are as follows: (1) We contribute a novel epidemiological dataset that describes the evolutionary process of the cluster of COVID-19 under the anti-contagion policies. (2) We propose a series of dynamic interaction network analysis methods to mine the evolutionary patterns of the cluster of COVID-19, which will provide useful information for governments making anti-contagion policies.

The rest of this paper is organized as follows. Section 2 gives the detail information about the dataset. In Section 3, we introduce how to conduct dynamic analysis and related findings. Section 4 presents our experimental results for simulating the

spread of the COVID-19 in the complex network. The paper summarizes the instructive conclusions in Section 5.

II. DATASET INFORMATION

A. Data acquisition and processing

The Beijing COVID-19 resurgent data comes from the notification issued by the Beijing Health Commission[1] since June 11. We collected this data manually and organize it in a specific format. The address information is divided into three categories including district-street-community. The location related to the confirmed COVID-19 patients is divided into the place of residence, the place of work, and the place of close contact that can be traced from the epidemiological investigation.

B. Statistical description

Initial COVID-19 cases in Beijing may be caused by an imported source of infections.[14] There are together 368 cases of COVID-19 infection were reported in Beijing from June 11 to July 12 at 24:00. Among them, 335 people were confirmed cases and 33 were asymptomatic infections. Among the 368 cases of infection, 73.9% (272) cases had a history of direct exposure (mainly including practitioners, staff and market visitors), and 25.6% (94 cases) were indirectly related cases.

As of July 5, Beijing Health Commission has released epidemiological information about 284 cases. Based on the analysis of gender, age and occupational composition of reported cases, the ratio of male cases to female cases is not much different, 42%, and 58% respectively. The risk of infection is slightly higher in the female population; the average age of the cases was 40.88 and 43.2 years old respectively; the occupations of the cases are mostly concentrated in the relevant personnel in the Xinfadi Market, accounting for 51.05% (145 people); the second reason for the infection of the cases is mainly concentrated in the catering personnel who may purchase goods from Xinfadi Market, and the people who had purchase behavior from the Xinfadi Market, accounting for 24.29% (69 people). According to the characteristics of population flow and migrant workers, mainly young and middle-aged people, have become the main source of imported cases in Beijing.

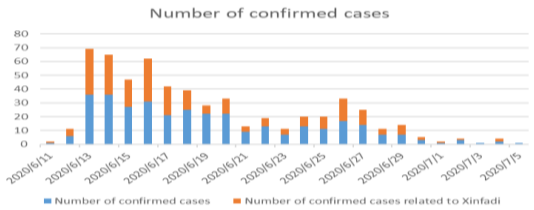

Fig. 1: Change of the number of daily confirmed infection cases and confirmed cases related to the Xinfadi Market.

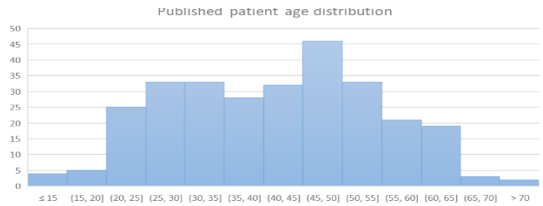

Fig. 2: Age distribution of confirmed cases

Besides, we present the construction method and temporal changes of the dynamic interaction networks in Section 3.

C. Cluster cases of COVID-19

A total of 29 clustered epidemic events related to Xinfadi involved 127 confirmed patients and asymptomatic infections. In this subsection, we discuss three different types of case studies including family clustered epidemic events, workplace clustered epidemic events, hybrid clustered epidemic events.

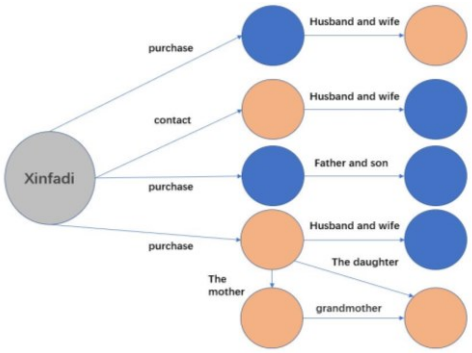

Fig. 3: Four family clustered epidemic events

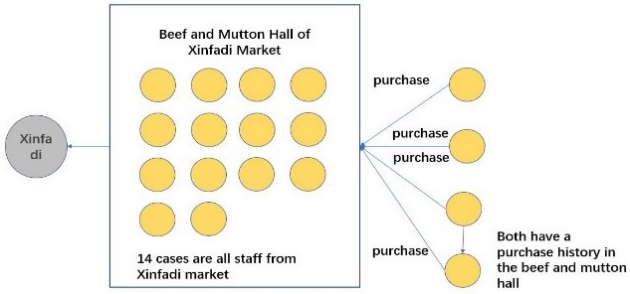

Fig. 4: Cases-1 of workplace clustered epidemic events

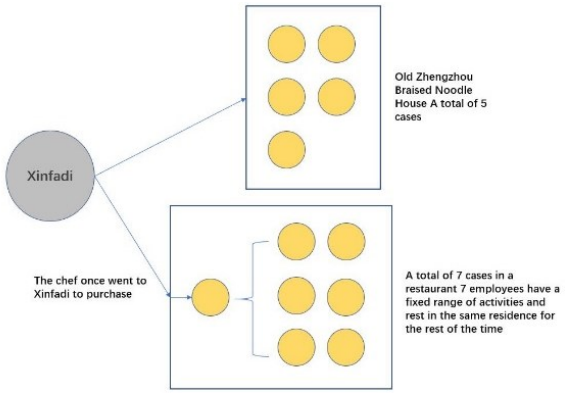

Fig. 5: Cases-2 of workplace clustered epidemic events

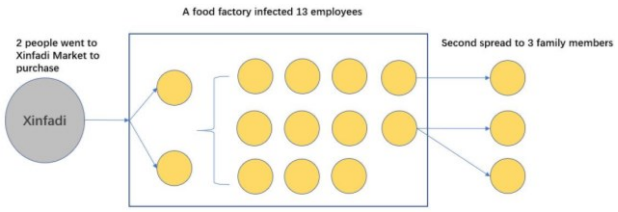

Fig. 6: Cases-3 of workplace clustered epidemic events

1. http://wjw.beijing.gov.cn/wjwh/ztzl/xxgzbd/

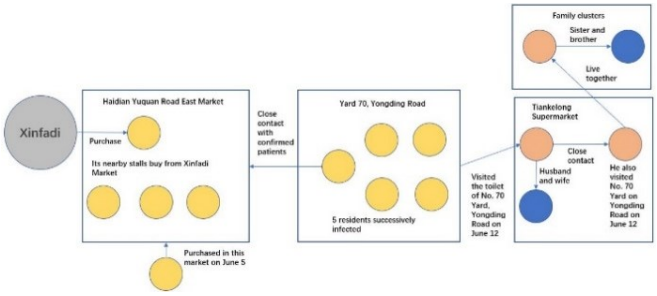

Fig. 7: Typical case of Hybrid clustered epidemic events

We can see that the structure of most family clustered epidemic cases is relatively simple. The spread path within the family is shorter. If quarantine measures are taken in time, large-scale family clustered epidemic spread will not happen.

Most of the workplace clustered epidemic events are related practitioners in the catering industry. The workplace which they work on is relatively closed and frequent contact. When the isolation measures are taken in time, the propagation path is relatively short.

Hybrid clustered epidemic events have a longer spread path and are closest to the transmission path of a true world epidemic outbreak without control measures. It contains situations such as family gatherings, workplace gatherings, and public gatherings alternate. The probability of epidemic spread is significantly higher in the places where people are in close contact.

III. DYNAMIC INTERACTION NETWORK CHARACTERISTICS ANALYSIS

Simply, we treat people and places as nodes, their interactions as edges, and build a complex network of COVID-19. We take personnel, personnel residence, work location, and close contact area as the nodes. The interaction between people and location, people and people, and the connection between location and location from the trajectory confirmed cases is the side to build an epidemic spreading network. The personnel are infected cases and asymptomatic infected persons. The address information is divided into three categories including district-street-community. The location related to the confirmed COVID-19 patients is divided into the place of residence, the place of work, and the place of close contact that can be traced from the epidemiological investigation.

Close contact areas are important locations announced in the epidemiological investigation of patients or contact cases. The edge between a place and a place indicates that the patient has a flow trajectory between the two places. And an edge is established at two levels between the patient and the street node of the work or between life place and the specific address of the work and living place. In this way, an epidemic spreading network is formed. With the development of the COVID-19, the network evolves. At time t, we denote V_t as the set of nodes in the network, and E_t as is the set of edges in the network. $G_t = (V_t, E_t)$ denote the interaction network at time t.

We according to data collected from June 11th to July 4th. starting from June 12th, at the interval of each publication of the survey results, use python's NetworkX related packages to construct network diagrams, and analyze network changes.

In order to explore the dynamic changes of the epidemic spreading network, we calculated the changes of different network characteristics in the spreading network of the epidemic.

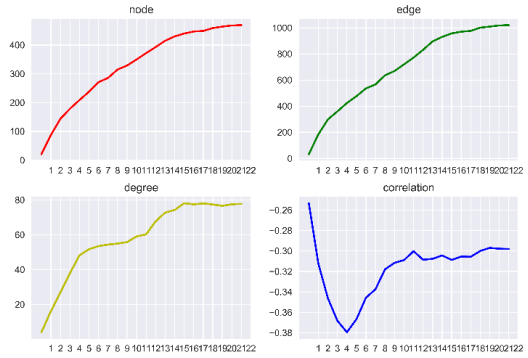

Fig. 8: The number of nodes, edges, the average degree, and the change curve of the correlation coefficient of the network at different time

The following figure shows some basic network changes, which are the number of nodes, the number of edges, the degree, and the classification coefficient. Fig. 8 shows how network characteristics have changed. The growth of the number of nodes and edges gradually slow down until its stop. The degree has a volatile growth in the middle period. The correlation coefficient quickly decays and then rises. But it is always at the level of negative correlation.

A. Network density

The density for undirected graphs is

$$d_t = \frac{2m_t}{n_{t(n_t-1)}} \quad (1)$$

Where n is the number of nodes and m is the number of edges in G. According to the definition, the network density ranges from [0,1]. The greater the network density, the more connections exist in the network, the higher the accessibility.

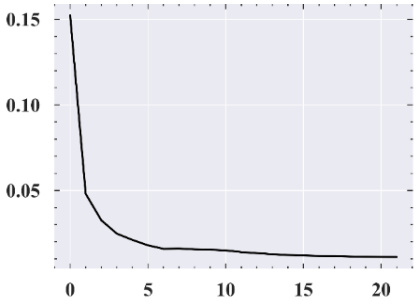

Fig. 9: daily changes in network density.

The network density is gradually decreasing, indicating that the spread of the epidemic is gradually decreasing, and the network connectivity of the epidemic is getting worse.

B. Betweenness centralization in network

Betweenness centrality of a node v is the sum of the fraction of all-pairs shortest paths that pass through v.Referred to as $C_b$tw, Calculated as follows:

$$C_{btw}(v) = \sum_{(s,p \in N_t)} \frac{\sigma_{(s,p)}(v)}{\sigma_{(s,p)}} \quad (2))$$

$\sigma_{(s,p)}$ is the number of shortest paths between node s_t and node p_t. $\sigma_{(s,p)}(v_t)$ is the number of shortest paths between node s and node p_t through node v.

Betweenness centralization is the gap between the centrality of the node with the highest centrality in the network and the centrality of other nodes. The greater the gap between this node and other nodes, the higher the betweenness centralization of the network. Betweenness centralization C_{B_t}:

$$C_B = \frac{\sum_{v \in N_t} max(C_{btw}) - C_{btw}(v)}{|N_t| - 1} \quad (3)$$

Intermediary centrality reflects the ability of nodes to occupy key positions in the network and their control over the network. The betweenness centrality of the overall network is related to the betweenness centrality of nodes. When the gap between the centrality of nodes is larger, the centrality of the network is greater.

We can see from Fig. 10 that after the outbreak of the epidemic began to detect, the intermediary centrality fluctuated first and then increased, maintaining a relatively high level and finally decreasing slightly. This shows that the epidemic has always revolved around certain key nodes, such as Xinfadi, with a high degree of aggregation.

In order to explore the key nodes, we calculate the daily top 5 of the intermediary centrality values of the following locations nodes. It shows in Fig. 11.

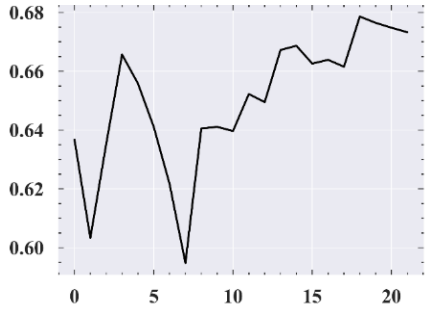

Fig. 10: Epidemic network intermediary centrality change over time

Most of the cases are closely related to the Xinfadi Market, Fengtai District, and Huaxiang. The intermediary center potential of these nodes is larger, which indicate that they have greater network control.

Xinfadi Market	0.707895	Huaxiang	0.147368	Yuetan Jiedao	0.1	Changyang town	0.1	Xiluoyuan Street	0.1
Xinfadi Market	0.622989	Huaxiang	0.328795	Fengtai District	0.184177	Lugouqiao Street	0.130001	Yuetan Jiedao	0.109596
Xinfadi Market	0.648389	Huaxiang	0.309282	Fengtai District	0.227516	Lugouqiao Street	0.086794	Yuetan Jiedao	0.06796
Xinfadi Market	0.675313	Huaxiang	0.291085	Fengtai District	0.191751	Lugouqiao Street	0.070985	Yuetan Jiedao	0.05491
Xinfadi Market	0.663888	Huaxiang	0.306307	Fengtai District	0.176296	Lugouqiao Street	0.067461	Lugouqiao	0.051885
Xinfadi Market	0.648743	Huaxiang	0.316632	Fengtai District	0.189616	Lugouqiao Street	0.083972	Lugouqiao	0.0515
Xinfadi Market	0.628905	Huaxiang	0.337507	Fengtai District	0.18004	Lugouqiao Street	0.070897	Huangcun town	0.061261
Xinfadi Market	0.602204	Huaxiang	0.336058	Fengtai District	0.183756	Lugouqiao	0.07343	Lugouqiao Street	0.07138
Xinfadi Market	0.647009	Huaxiang	0.275302	Lugouqiao	0.114651	Fengtai District	0.08589	Huangcun town	0.075172
Xinfadi Market	0.647116	Huaxiang	0.269979	Lugouqiao	0.108727	Huangcun town	0.079231	Fengtai District	0.076933
Xinfadi Market	0.645214	Huaxiang	0.27749	Lugouqiao	0.111937	Huangcun town	0.071314	Fengtai District	0.067836
Xinfadi Market	0.657161	Huaxiang	0.242953	Haidian District	0.086956	Lugouqiao	0.072718	Huangcun town	0.063759
Xinfadi Market	0.654003	Huaxiang	0.253046	Haidian District	0.082499	Lugouqiao	0.068761	Huangcun town	0.060528
Xinfadi Market	0.671264	Huaxiang	0.244226	Haidian District	0.078196	Daxing District	0.054592	Xihongmen Town	0.053486
Xinfadi Market	0.672544	Huaxiang	0.2412	Haidian District	0.075582	Daxing District	0.058567	Huangcun town	0.057037
Xinfadi Market	0.666357	Huaxiang	0.250804	Haidian District	0.07378	Daxing District	0.05721	Huangcun town	0.055663
Xinfadi Market	0.667605	Huaxiang	0.245786	Haidian District	0.072696	Daxing District	0.062857	Xihongmen Town	0.05882
Xinfadi Market	0.66524	Huaxiang	0.248211	Haidian District	0.072458	Daxing District	0.062533	Xihongmen Town	0.058553
Xinfadi Market	0.681881	Huaxiang	0.240074	Daxing District	0.061661	Xihongmen Town	0.057269	Huangcun town	0.05327
Xinfadi Market	0.679781	Huaxiang	0.239438	Daxing District	0.060839	Xihongmen Town	0.056646	Huangcun town	0.052588
Xinfadi Market	0.678088	Huaxiang	0.242728	Daxing District	0.060109	Xihongmen Town	0.056087	Huangcun town	0.052108
Xinfadi Market	0.676549	Huaxiang	0.245868	Daxing District	0.059945	Xihongmen Town	0.055974	Huangcun town	0.051967

Fig.11: daily top 5 of the intermediary centrality values of Location node

C. *Compare with other networks*

Small-world network makes information spread quickly in nodes. It shows high aggregation and good accessibility. Network performance can be rapidly changed by changing the relationship between a few nodes in the small-world network. It is mainly measured by the average path length and clustering coefficient.

The average path length is the average of the shortest paths between all pairs of nodes in the network. Some literature such as [15] shows that for an infectious disease network with the same number of nodes, the longer the average path length, the slower the spread of the epidemic. The clustering coefficient characterizes the probability of interconnection between nodes the higher the aggregation coefficient is, the closer the network connection is.

Here we generate an ER network with the same number of nodes and the probability for edge creation is 0.3.ER network is the Erdős–Rényi random graph model. WS network is the small-world graph Contains the same number nodes, each node has the same number of neighbors as the original network average neighbors, randomizes the reconnect edge with probability 0.3. BA network is a random scale-free network generated by the Barabási–Albert model. ER network, WS network, and BA network are compared with the real epidemic transmission network. To observe its small-world characteristics.

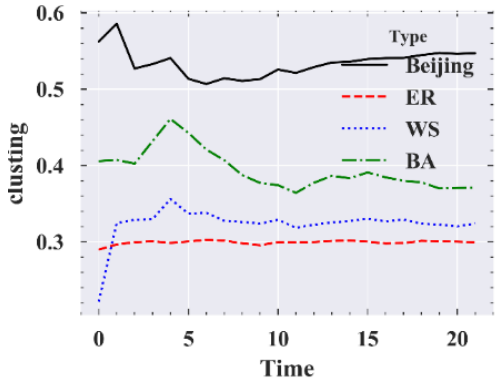

Fig. 12: Clustering coefficient of different networks changes at different times

The COVID-19 Beijing spread network of epidemic situations presents certain characteristics of the small-world.

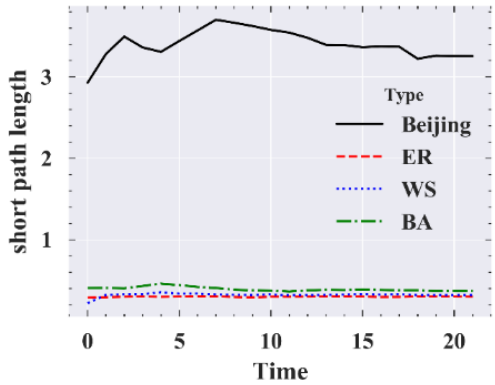

Fig. 13: Shortest path length of different networks changes at different times

IV. Simulation Analysis

Wei et al. [16] used the SEIR dynamics model to fit COVID-19 epidemic in Beijing's daily onset infections. To further explore the influence of different network structures on the transmission speed and mode of such sudden cluster epidemics. We use the SIR model in two different types of networks to simulate the spread of infectious diseases.

It can be observed from the spread of cases that if isolation measures are taken promptly, family-type, or workplace-type gathering cases. The network structure is closer to the BA scale-free network with fewer edges. Fig. 14 is an example of the BA scale-free network with fewer edges.

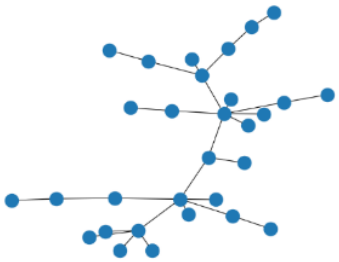

Fig. 14: BA scale-free network with fewer edges

We use a BA scale-free network with 300 nodes and 300 edges to simulate home and workplace aggregation. The blue node is the uninfected node, and the green node is the recovered node. The red node is the infected node. Randomly select 10 nodes to initialize as infected persons. Take thirty days as the propagation time. Observe the network changes after that. Thirty days later, only some nodes have been infected with COVID-19.

Max_deg_I record max number of neighbors within infected. tot_deg_I records the total number of neighbors within infected. Figure 10 shows the sir model change in the number of infections.

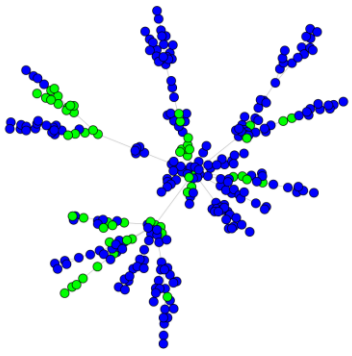

Fig. 15: Infection status of BA scale-free network after 30 days

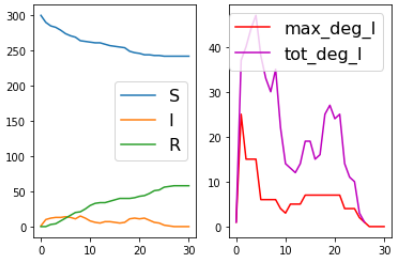

Fig. 16: Changes of SIR infections on the BA scale-free network

Figure 16 depicts that SIR model changes in where the spread structure is closer to family clustered epidemic events which under timely control measures. However, if control measures are not taken in time to prevent a mixed type of aggregation that develops into a diffusion state. The network structure is closer to a random network or a small world network as Fig. 17.

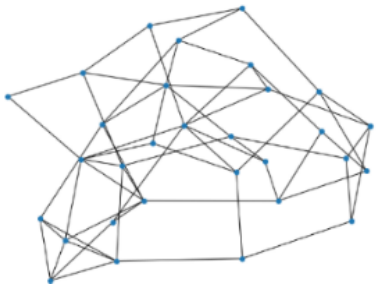

Fig. 17 A small world network example

A small-world network with 300 nodes, 4 neighbors per node, and a randomized reconnection probability of 0.5 is used as a simulation network to modeling the COVID-19 spread. We still select 10 nodes to initialize as infected persons and observe the changes after 30 days. Most nodes have been infected or infected with COVID-19.

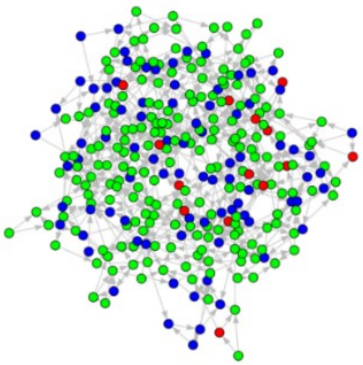

Fig. 8: Infection status of a small world network after 30 days

Fig. 19 shows the change in the number of infections in the SIR model under this network structure. Compared to Fig. 16. The number of people infected has increased by more than 150 percent. Limiting contact can reduce the rate of spread, it is consistent with some previous studies[2, 16].

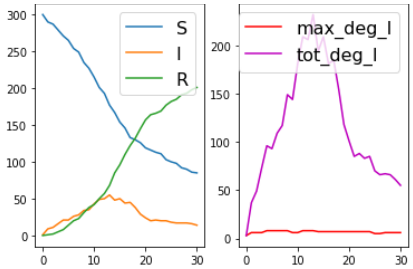

Fig. 19: Changes in the number of SIR infections on the small world network

V. CONCLUSION

Leveraging the self-build dataset about the spread of COVID-19 at the Xinfadi Market in Beijing, we analyzed the evolutionary characteristics of the cluster of COVID-19 under anti-contagion policies. Excluding the volatilities of some evolutionary characteristics in the early stage of the outbreak due to incomplete information from epidemiological investigations, we make the following remarkable conclusions:

(1) The overall connection density of the network is low, and its topological characteristics are in a trend of rapid changes in the early stage, and gradually fall back to a stable trend after a certain period of time. In the epidemic network, the number of edges is increasing and the shortest path is not increasing simultaneously. These results shows that the COVID-19 epidemic networks have a small spread area and the control measures for the epidemic situation are effective.

(2) The dynamic epidemic networks present certain small-world and scale-free characteristics. Most of the nodes are related to Xinfadi Market or Huaxiang Street. And the COVID-19 spread network has an obvious aggregation, forming two central spread areas around Xinfadi Market and Huaxiang Street. Daxing District and its subordinate streets are several region with relatively high degree values, indicating that during the incubation period of COVID-19, it is necessary to take priority interventions policy in the areas with large population mobility.

(3) The simulation results indicate that the propagation speed and scale of the family clustered epidemic, and the epidemic network will reduce to nearly one-fifth of the propagation scale of the mixed aggregation under the condition of timely isolation. This provides a remarkable insight that reducing the contact and early control significantly and substantially slow the spread.

We argue that these findings can provide significant insights for policymakers and researchers to understand the evolutionary characteristics regarding the cluster COVID-19 and deploy effective anti-contagion policies.

ACKNOWLEDGMENT

This work is supported by the Ministry of Health of China under Grant No.: 2017ZX10303401-002 and 2017YFC1200302, and the Natural Science Foundation of China under Grant No.: 71472175, 71602184 and 71621002 and 71974187, and the National Key Research and Development Program of China under 2016QY02D0305.

REFERENCES

[1] S. Hsiang, D. Allen, S. Annan-Phan, K. Bell, I. Bolliger, T. Chong, H. Druckenmiller, L. Y. Huang, A. Hultgren, and E. Krasovich, “The effect of large-scale anti-contagion policies on the COVID-19 pandemic,” Nature, pp. 1-9, 2020.

[2] M. Chinazzi, J. T. Davis, M. Ajelli, C. Gioannini, M. Litvinova, S. Merler, A. P. y Piontti, K. Mu, L. Rossi, and K. Sun, “The effect of travel restrictions on the spread of the 2019 novel coronavirus (COVID-19) outbreak,” Science, vol. 368, no. 6489, pp. 395-400, 2020.

[3] G. Csardi, and T. Nepusz, “The igraph software package for complex network research,” InterJournal, complex systems, vol. 1695, no. 5, pp. 1-9, 2006.

[4] G. Liu, Y. Wang, and M. A. Orgun, "Optimal Social Trust Path Selection in Complex Social Networks." pp. 1397-1398.

[5] X. Jin, and Y. Wang, “Research on social network structure and public opinions dissemination of micro-blog based on complex network analysis,” Journal of Networks, vol. 8, no. 7, pp. 1543, 2013.

[6] G. Li, J. Hu, Y. Song, Y. Yang, and H.-J. Li, “Analysis of the terrorist organization alliance network based on complex network theory,” IEEE Access, vol. 7, pp. 103854-103862, 2019.

[7] M. E. Newman, “The structure of scientific collaboration networks,” Proceedings of the national academy of sciences, vol. 98, no. 2, pp. 404-409, 2001.

[8] J. Zhou, A. Zeng, Y. Fan, and Z. Di, “Identifying important scholars via directed scientific collaboration networks,” Scientometrics, vol. 114, no. 3, pp. 1327-1343, 2018.

[9] H. A. M. Malik, A. W. Mahesar, F. Abid, and M. R. Wahiddin, "Two-mode complex network modeling of dengue epidemic in Selangor, Malaysia." pp. 1-6.

[10] H. MALIK, A. Waqas, F. Abid, A. GILAL, A. MAHESSAR, and Y. Koondar, “Complex network of dengue epidemic and link prediction,” Sindh University Research Journal-SURJ (Science Series), vol. 48, no. 4, 2016.

[11] F. Brenner, and N. Marwan, “Change of influenza pandemics because of climate change: Complex network simulations,” Revue d'Épidémiologie et de Santé Publique, vol. 66, pp. S424, 2018.

[12] B. Hu, J. Gong, J. Sun, and J. Zhou, “Exploring the epidemic transmission network of SARS in-out flow in mainland China,” Chinese Science Bulletin, vol. 58, no. 15, pp. 1818-1831, 2013.

[13] B. Hu, J. Gong, J. Zhou, J. Sun, L. Yang, Y. Xia, and A. N. Ibrahim, “Spatial-temporal characteristics of epidemic spread in-out flow—Using SARS epidemic in Beijing as a case study,” Science China Earth Sciences, vol. 56, no. 8, pp. 1380-1397, 2013.

[14] W. Tan, P. Niu, X. Zhao, Y. Pan, Y. Zhang, L. Chen, L. Zhao, Y. Wang, D. Wang, and J. Han, “Reemergent Cases of COVID-19—Xinfadi Wholesales Market, Beijing Municipality, China, June 11, 2020,” China CDC Weekly, vol. 2, no. 27, pp. 502-504, 2020.

[15] P. Block, M. Hoffman, I. J. Raabe, J. B. Dowd, C. Rahal, R. Kashyap, and M. C. Mills, “Social network-based distancing strategies to flatten the COVID-19 curve in a post-lockdown world,” Nature Human Behaviour, pp. 1-9, 2020.

[16] Y. Wei, J. Guan, Y. Zhao, S. Shen, and F. Chen, “Inference of start time of resurgent COVID-19 epidemic in Beijing with SEIR dynamics model and evaluation of control measure effect,” Zhonghua liu Xing Bing xue za zhi= Zhonghua Liuxingbingxue Zazhi, vol. 41, pp. E077-E077, 2020.